Magnetic Resonance Imaging, Vol. 4, pp. 229–235, 1986
Printed in the USA.

0730–725X/86 $3.00 + .00

● *Original Contribution*

TISSUE CONTRAST ENHANCEMENT: IMAGE RECONSTRUCTION ALGORITHM AND SELECTION OF TI IN INVERSION RECOVERY MRI

P. R. Moran, Ph.D., N. G. Kumar, Ph.D., N. Karstaedt, M.B., B.Ch., and S. C. Jackels, Ph.D.

Department of Radiology, Bowman Gray School of Medicine, Wake Forest University, 300 S. Hawthorne Road, Winston-Salem, North Carolina 27103

It is clearly demonstrated that the proper application of the inversion recovery imaging pulse sequence is dependent on the method of image reconstruction and the selection of TI for optimum tissue contrast. There are two methods of 2DFT image reconstruction of IR sequence time-domain raw data. The first is a modulus-image reconstruction algorithm (contrast-obliterating option), and the second is a phase-correction routine for reconstructing "phase-sensitive" true IR-images. The second option generates proper "in-phase" images, retains proper scale of contrast, but can invert the algebraic sign of image-values under certain conditions. A series of "phase-sensitive" and "modulus" reconstructed brain images, obtained with conventional and optimized new IR pulse sequences, are shown to demonstrate these effects. They illustrate the considerable advantages gained, in practical clinical situations, if one generates "phase-sensitive" true IR-images from IR-sequence raw data at optimum TI for tissue contrast enhancement.

Keywords: **MRI, Tissue contrast enhancement, Image reconstruction algorithm, Inversion recovery MRI, Optimized new IR pulse sequences.**

INTRODUCTION

The inversion recovery (IR) pulse sequence has excellent potential advantage for T_1 contrast differentiation because the magnetization range is twice that of the saturation recovery (SR) sequence. The signal from IR is therefore twice that available from the SR sequence. Also, it is well known that T_1 sensitivity with SR depends greatly upon precisely adjusted excitation profiles in the selective-excitation process.[1–3] The IR sequences have much less sensitivity-degradation caused by small-angle excitations in the wings of the slice profiles. However, several problems with the proper application of IR imaging have hindered its potential from being realized.[4–6]

First, there are two methods of 2DFT (two-dimensional Fourier transform) image reconstruction of IR sequence time domain raw data. The "real" or "phase-sensitive" method preserves the algebraic sign of the observable magnetization which can be either positive or negative in IR data. The other method, "magnitude" or "modulus," displays only the magnitude of the magnetization, thus making all signals positive. There are fundamental differences with the two types of image reconstruction algorithms and in the IR images generated with the two modes of reconstruction, yet the literature almost never specifies the method of reconstruction for IR images. Second, equations based upon an assumption of one mode of reconstruction have been presented as generally applicable to IR images.[7] Thus, there is confusion concerning the contrast capability, the optimum pulse intervals and the relation between T_1 and signal intensity in inversion recovery imaging.

Several recent papers have dealt with the effects of pulse interval selection on image contrast in IR images generated using each method of reconstruction. Young, Bailes, and Bydder[8] noted the "anomolous" relationship between signal intensity and T_1 in images with short TI and modulus reconstruction. Hendrick, Nelson and Hendee[9] point out the contrast loss that is incurred in IR images generated with modulus reconstruction. They also observe that in some cases the region of contrast loss in modulus—reconstructed images coincides with the region of maximum contrast differentiation for the same image produced with the real reconstruction method. Thus, it is clear that the

RECEIVED 5/12/85; ACCEPTED 12/5/85.
Address Correspondence to P. R. Moran or N. G. Kumar, Department of Radiology, Bowman Gray School of Medicine, 300 S. Hawthorne Road, Winston-Salem, North Carolina 27103

proper application of the IR sequence is dependent upon the method of reconstruction being used and in most cases real reconstruction gives superior results.

The purpose of this paper is to develop the appropriate physical theory of both image reconstruction methods relevant to IR sequences and to present a comparison of the conventional and optimized new IR pulse sequences for brain for tissue contrast enhancement in order to demonstrate that the inversion recovery pulse sequence has excellent capability for high level of T_1 contrast differentiation with proper selection of TI and image reconstruction method. We will then summarize for each 2DFT image reconstruction method the relationship between pulse interval (TI) and contrast observed in the images in order to show that the selection of optimum TI for tissue contrast is highly dependent upon the reconstruction method (Fig. 1). Finally, a series of "phase-sensitive" and "magnitude" reconstructed brain images from the same raw data, obtained with conventional (IR400, Fig. 2) and modified new IR pulse sequences at optimum TI (IR250 and IR225; Figs. 3 and 4), are shown to demonstrate these effects; they illustrate the considerable advantages gained, in practical clinical situations, from the proper application of the inversion recovery imaging pulse sequence.

METHODS

The images were obtained on a Picker resistive magnet imaging system operating at a magnetic field strength of 0.15 Tesla and proton observation frequency of 6.3855 MHz. The transmitter provides RF pulses at the center (Larmor) frequency ($f_0 = \gamma/2\pi B = 6.3855$ MHz). For the 0.15 T system, the synthesizer frequency is 21.3855 MHz and the reference (carrier) frequency is 15 MHz.

The Picker software includes routines for generating computed T_1 and T_2 images. The T_1 image is computed from an IR and a SE image having the same TR (sequence repeat time) and TE (echo formation time) values. The ratio of the IR and SE pixel intensities is approximately given by

$$S = \frac{N_{IR}}{N_{SE}} = \frac{[1 - 2\exp(-TI/T1) - \exp(-TR/T1) + 2\exp(-(TR - TE/2)/T1)]}{[1 + \exp(-TR/T1) - 2\exp(-(TR - TE/2)/T1)]}. \quad (1)$$

In Eq. 1, S is a function of the pulse sequence parameters and T_1. A look up table for T_1 based on the S-values is generated and used to determine T_1 from the value of S at each pixel location. A similar algorithm is used for the T_2 computed image. Two spin-echo sequences with the same TR but different echo formation times, TE_1 and TE_2, are required. The ratio of the SE pixel values is given approximately by

$$S = \frac{N_{SE1}}{N_{SE2}} = \frac{(1 - 2\exp \cdot ((-TR + TE1/2)/T_1) + \exp(-TR/T_1)}{(1 - 2\exp \cdot ((-TR + TE2/2)/T_1) + \exp(-TR/T_1)} \cdot \frac{\exp(-TE1/T_2)}{\exp(-TE2/T_2)}. \quad (2)$$

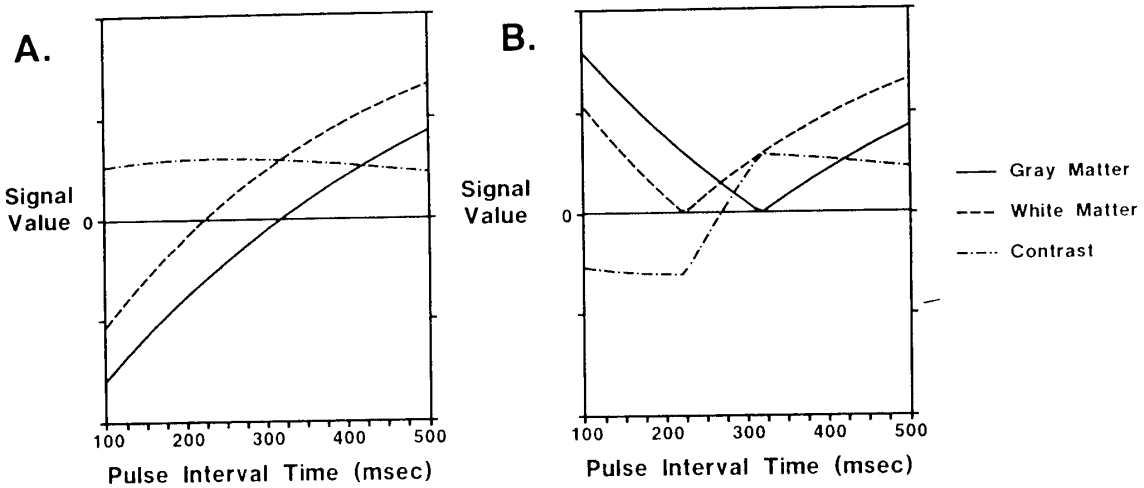

Fig. 1. Shows the calculated signal as a function of TI using the NMR parameters (TR = 2200, TE = 40 msec, Table 1) measured on the brain of a volunteer. Also shows the contrast between the two tissues, $S_W - S_G$. (A) "Real" reconstructed signal. (B) "Magnitude" reconstructed signal.

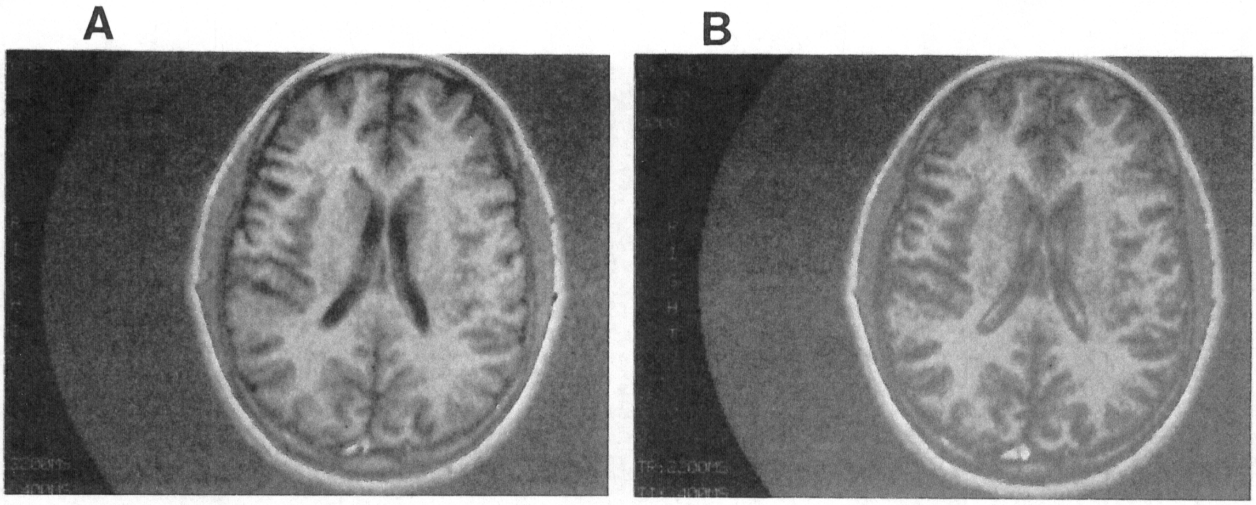

Fig. 2. The conventional IR 400 pulse sequence for brain (TI = 400 msec). (A) "Phase-sensitive" image. (B) "Magnitude" image. Both the images were reconstructed from the same time domain raw data. Note the absence of good tissue contrast between white and gray matter even in the true IR-image (A).

An approximate solution of the above equation used for T_2 computation is

$$T_2 = \frac{\text{TE2} - \text{TE1}}{\ln S}. \qquad (3)$$

The NMR parameters (Table I), used in the calculated signal as a function of TI (Fig. 1), were measured on the brain of a normal volunteer from the computed T_1 (Fig. 5), T_2 and proton density images. The T_1 image (Fig. 5) was computed from IR400 and SE20 (TE = 40 msec) having the same TR (2200 msec) and TE (40 msec) values. The T_2 image was computed from SE20 (TE_1 = 40 msec) and SE40 (TE_2 = 80 msec) spin echo sequences with the same TR, and the proton densities were derived from the calculated T_2-values and the SE15 spin-echo sequence images with TE of 30 msec and long TR of 2200 and 3000 msec.

The conventional IR400 (Fig. 2), and the optimized IR250 (Fig. 3) and IR225 (Fig. 4) brain images are of the same volunteer imaged in the transverse section using a spin-echo readout (TE = 40 msec). The images were reconstructed using two-dimensional Fourier transform (2DFT) of two repetitions of 256 data lines (multislice, slice thickness = 10 mm, bandwidth = 10

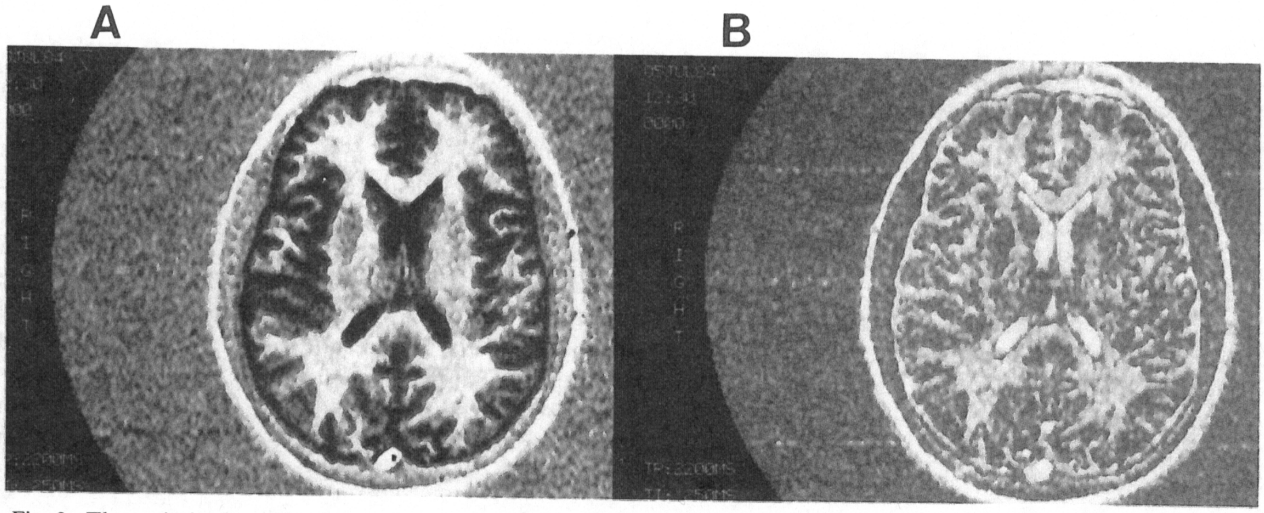

Fig. 3. The optimized new IR-250 pulse sequence for brain for tissue contrast enhancement at the optimum TI of 250 msec. (A) "Phase-sensitive" reconstructed image using the phase correction routine to give an "in-phase" true IR-image. Note the high level of tissue contrast between white and gray matter as compared to the conventional IR 400 image (2A). (B) shows "modulus" image reconstruction of the same raw data. Note the dramatic loss of tissue contrast and the appearance of many "modulus" artifacts.

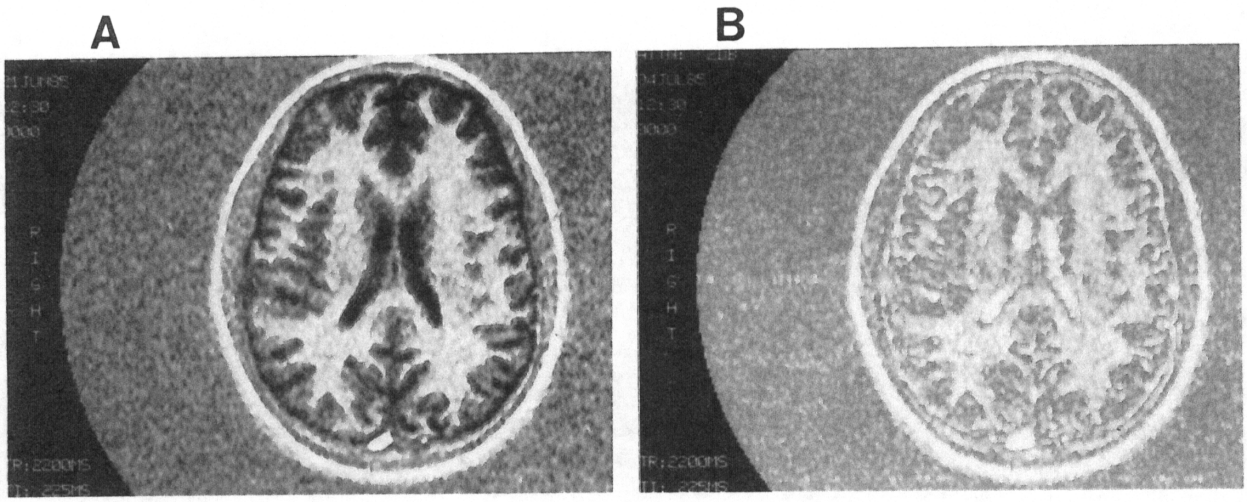

Fig. 4. The modified new IR 225 pulse sequence (TI = 225 msec). (A) shows phase-sensitive true IR-image. With high level of tissue contrast resolution. (B) Modulus reconstructed image from the same raw-data showing many modulus artifacts and considerable loss of tissue contrast.

KHz, TR = 2200 msec, resolution = 256 × 256, pixel size = 1.17 mm, line pairs/cm = 4.27). Both the "phase-sensitive" and "modulus" images were reconstructed from the same time domain raw data.

RESULTS AND DISCUSSION

Mathematical Basis of IR Reconstructions

Most MR imagers use a spin-echo readout appended to the initial IR sequence which is:

$$180° - \text{TI} - 90° - \tau - 180° - \tau - \text{Echo} - \text{centroid}$$

$$\text{TE} = 2\tau \text{ or } \tau = \text{TE}/2$$

When TE is very short compared to TR, the magnetization excited by the readout pulse is given by the expression:

$$\langle M_t \rangle = M_0[1 - 2\exp(-\text{TI}/T_1) + \exp(-\text{TR}/T_1)]\exp(-\text{TE}/T_2) \quad (4)$$

This precessing magnetization induces an emf in the receiver coils, which is amplified in rf receiver stages and combines with reference carrier frequency from the synthesizer oscillator in a two channel quadrature phase sensitive detector. The reference signals of the two identical phase sensitive detectors differ by 90°, thereby allowing discrimination between higher $(B_0 + \Delta B_0)$ and lower $(B_0 - \Delta B_0)$ frequencies (above and below resonance) via phase changes with respect to a given reference frequency in the time domain. Spatial encoding of the resulting output channels is achieved by activating various cycles of imaging gradient applications. The in-phase channel is called the I-channel (or real channel) signal, and the quadrature-phase reference channel is called the Q-channel (or imaginary channel) signal. Together these form, from a single data-cycle, a single line in Fourier-representation space of the subject distribution of the magnetization of Eq. 4. A full discussion has been given elsewhere.[10]

It is necessary to understand that physical effects related to the pulsing of gradient field coils, electronic pecularities, quadrature mismatch of the channels, etc., can produce various phase shifts of the data outputs. These phase shifts do not depend upon the subject spatial distribution, but typically are global phase errors. The result is that the I-channel and Q-channel may have a constant phase rotation characterizing them, so that the I-channel actually carries a large component of quadrature-phase magnetization signal and the Q-channel correspondingly carries in-phase magnetization signal. Moreover, the center of the data collection and digitization window applied to the signal readout may have a timing shift from the actual spin-echo centroid position. The former produces a spatially independent phase shift in the recon-

Table 1. NMR parameters of volunteer subject

	T_1 (msec)	T_2 (msec)	Relative proton density
White matter	322	84	0.92
Gray matter	465	96	1.0

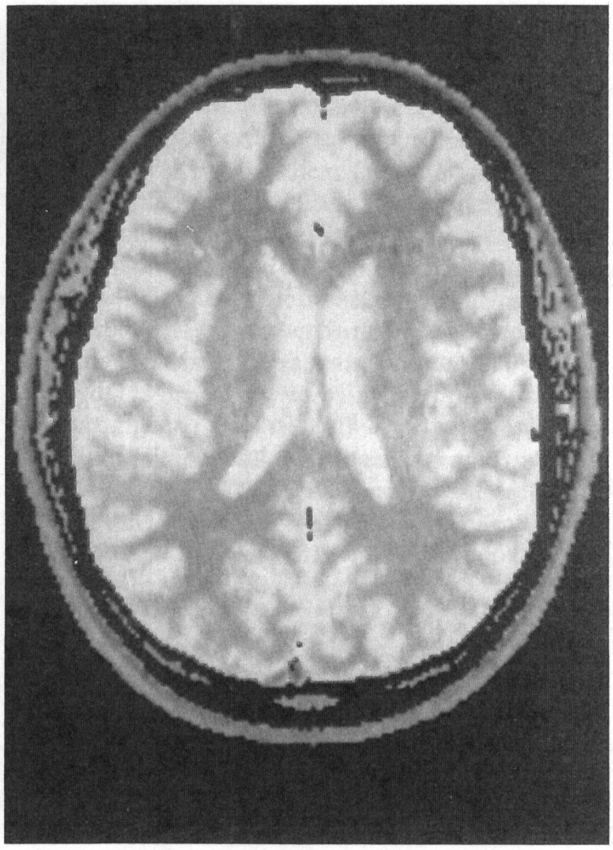

Fig. 5. Computed T_1 brain image of the same volunteer as above (see Methods section for details). The bright areas correspond to long T_1.

structed linear images and the latter produces a spatially oscillatory phase shift across the field of view (a fixed temporal shift in data space).

There are two ways to approach removing the effects of such spurious phase shifts. We need initially to realize that, from the I-channel and Q-channel signal data outputs, one reconstructs two linear images by some variation of Fourier transform algorithm.[10,11] These images are called the I-image and the Q-image; that is, the total linear image reconstructed initially, J(x, y, z), can be described as a complex image pair as shown below.

$$J(x, y, z) = I(x, y, z) + iQ(x, y, z) \qquad (5)$$

However, to the extent that the I-channel and Q-channel data are rotated into each other by systematic phase errors, the I-image and the Q-image of Eq. 5 each contain in-phase and quadrature-phase magnetization components. For example, consider a phase shift, ϕ (phase angle), which is independent of spatial position (global) in the subject. Then the I(x, y, z) image reflects the magnetization distribution by

$$I(x, y, z) = \langle \text{in-phase } M_{subj}(x, y, z) \rangle \cos \phi + \langle \text{quadrature-phase } M_{subj}(x, y, z) \rangle \sin \phi \qquad (6)$$

The following conjugate result applies to the Q-image.

$$Q(x, y, z) = \langle \text{quadrature-phase } M_{subj}(x, y, z) \rangle \cos \phi - \langle \text{in-phase } M_{subj}(x, y, z) \rangle \sin \phi \qquad (7)$$

MODULUS RECONSTRUCTION

The first method of attempting to deal with the problem of instrumentally induced spurious phase shifts (phase errors) is based upon the assumption that *only* in-phase magnetization originally was excited, that the magnetization distribution in the subject is everywhere positive, and that anything to the contrary is not physically admissible. This is not true, in general, since phase modulation information can be essential in some applications.[12,13] The most important aspect in our current concern is that the magnetization described by Eq. 4 can be both positive and negative. In this case, the negative magnetization at some location (not having yet recovered through zero during the interval TI) corresponds to π-out-of-phase precessing magnetization. Nevertheless, the modulus reconstruction algorithm effectively assumes the contrary: as a post linear reconstruction step, it forms the square root of the sum of squares of the I-image and the Q-image to give an "absolute-value of J(x, y, z)" image.

$$|J(x, y, z)| = [I^2(x, y, z) + Q^2(x, y, z)]^{1/2} \qquad (8)$$

When this algorithm is applied to IR sequence data, the resulting modulus array qualitatively is an image. However pixels that, in physical reality, should be negative (just as negative CT numbers occur in x-ray CT displays) are inverted to become positive MR numbers in the display. That is, positive values remain positive, but negative values also become positive (Fig. 1B). It is therefore not the ideal mode for inversion recovery sequence which is aimed at exploiting the enhanced T_1 contrast discrimination between tissues.

Consequently, modulus reconstruction has a fundamental effect on the contrast observed between two tissues. Figure 1 shows the "real" and "magnitude" reconstructed calculated signal for the white and gray matter plotted as a function of TI using the NMR parameters from Table I. The contrast between the two tissues, $S_W - S_G$, is also plotted in Fig. 1, the white matter having shorter T_1, T_2, and relative proton density than the gray matter. From the "magnitude" reconstructed curve (Fig. 1B) it can be clearly seen

that at TI values below the null point for white matter, gray matter is brighter than white matter, whereas at TI longer than the null point for gray matter tissue, the converse is true. Thus, in a clinical subject where there may be a relatively large range of T_1, there is ambiguity in the relationship between T_1 and brightness in modulus reconstructed images. Furthermore, between the two null points, the contrast changes rapidly from negative to positive and at some point passes through zero (Fig. 1B). Thus, a spurious conclusion that the two tissues in Fig. 1B have similar T1 values could be drawn if the data were collected in this TI range. These effects lead to significant loss of contrast resolution in modulus reconstructed IR images. An unsatisfactory attempt to remedy this problem has been to extend TI to such long values that no negative magnetization remains in the subject distribution. But at long TI delays, there is very little T_1 contrast discrimination because the magnetization of all tissues has recovered almost completely.

Phase-sensitive (Real) reconstruction (phase correction of data-channels). In this approach to phase error correction, one assumes that the subject distribution of magnetization is "Real." That is, the magnetization excited may have positive as well as negative values (1A), but it is all "in-phase" magnetization because the quadrature-phase excitation before gradient application is everywhere zero. It turns out that this assumption can be relaxed to the requirement that the phase shifts (apart from 180° inversions) are close to zero everywhere and average to zero globally.

There exists a theorem of Fourier transforms showing that the central-section transforms of any "Real" subject must be symmetric about zero frequency. This translates, in MR data, as follows: a central section line is a zero-encoded view in the so-called "2" or "3DFT" data strategies of any view in the radial gradient or polar gradient strategies.[10] If one forms the sum of the squares of the I-channel and the Q-channel output signals, the result must be symmetric about the position of the data centroid. In other words, the modulus of the data channels achieves a maximum or a minimum. One can search the modulus of the data channels and find the center by locating the point of zero slope.

One has now located the sample bin corresponding best to the spatial frequency origin, q = 0, which is the temporal "begin-FID" point at the echo center. Since the parent distribution is real, the correct Q-channel data must be antisymmetric about q-frequency origin (see ref 10), and this implies that the value of the Q-channel data at that point should be zero. If a global phase shift is present, then the observed Q-channel data is not zero. However, the ratio of the Q-channel value to the I-channel value (both at the determined centroid position) is the trigonometric tangent of the residual global phase shift, tan ϕ, in the notation of Eqs. 6 and 7. As is well known from trigonometry, one can determine the arctangent of the ratio (equal to ϕ) only modulo 180°.

Thus, while the global phase correction can be determined and the I-channel and Q-channel data recombined to "unrotate" the effect of the ϕ-error, the result may be incorrect by a minus sign. The standard phase correction algorithms assume that the phase shift so determined is that which produces an image whose values are positive *on the average.* Obviously, from Eq. 4, if the TI time is short enough, then the subject average magnetization has not relaxed through zero in the IR process. Thus the true signal received is negative after the 90°-rf-excitation. The effective phase is, on the average, 180° and not between ±90°. The result of phase correction in this case is to place a minus sign before M_0 in Eq. 4. Consequently, the algorithm inverts all true image values, positive becomes negative and negative becomes positive. This effect differs qualitatively from the "inversion" encountered in the modulus-reconstruction method where negative values become positive, but positive values remain positive (Fig. 1B).

We have observed that the conventional IR400 sequence for brain is relatively less effective in generating contrast between white and gray matter even in the "Real" reconstructed image (Fig. 2A) as compared to the optimized IR 250 and IR225 pulse sequences for brain.[14] The optimum TI for tissue contrast based on the NMR parameters of Table I and using the inversion recovery (with a rephasing pulse) equation of reference 9 calculates to be ~237 msec and is sensitive to T_1, T_2, and relative proton density. We iterated around this value (237 ± 13 msec) to generate optimized pulse sequences. It is clearly demonstrated in Fig. 3 that there is a high level of tissue contrast between white and gray matter in the "phase-sensitive" reconstructed image (Fig. 3A) and dramatic loss of contrast in the "magnitude" reconstructed image (Fig. 3B). The optimum TI at ~250 msec for maximum tissue contrast between white and gray matter in the "real" reconstructed curve (Fig. 1A) corresponds to a minimum tissue contrast at ~250 msec in the "magnitude" reconstructed curve (Fig. 1B). This demonstrates that the selection of optimum TI for tissue contrast is highly dependent on the image reconstruction method. The IR225 image (Fig. 4A) also exhibits a high level of tissue contrast resolution in the "phase-corrected" reconstructed image as compared to the conventional IR400 (Fig. 2A). Since T_1 exhibits B_0 dependence, selection of optimum TI and

TR for tissue contrast enhancement is dependent on the operating field strength of the individual scanner.

In going from IR400 and IR250, the calculated contrast enhancement of ~14% between white and gray matter (Fig. 1A) is in agreement with the observed ~18% enhancement (Fig. 3A) which translates into a high level of contrast between white and gray matter in the IR250 image. The clinical application of these optimized IR pulse sequences is under investigation and it remains to be seen if this tissue contrast enhancement of ~18% will aid in the detection and diagnosis of the diseased tissues.

CONCLUSION

The conventional IR400 sequence for brain is less effective in generating contrast between white and gray matter as compared to the optimized IR pulse sequences (IR250 and IR225) which exhibit high level of tissue contrast. The magnitude reconstruction is a nonlinear transform which generates only positive signal from magnetization which otherwise can be both positive and negative. There are also artifacts which result in substantial loss of contrast resolution and T_1 discrimination between tissues (Fig. 3B). On the other hand, it is shown in Fig. 3A that the "real" reconstruction results in substantial increase in resolution and in a high level of T_1 discrimination. The "phase-sensitive" image reconstruction is the ideal method for the inversion recovery imaging sequence which is aimed at exploiting the enhanced T_1 contrast discrimination between tissues. Thus, it is clear that the proper application of the IR imaging sequence is dependent on the method of image reconstruction and the selection of TI for maximum tissue contrast.

REFERENCES

1. Edelstein, W.A.; Bottomley, P.A.; Hart, H.R.; Smith, L.S. Signal, noise and contrast in NMR imaging. *J. Comput. Assist. Tomogr.* 7:391–401; 1983.
2. Rosen, B.R.; Pykett, I.L.; Brady, T.J. Spin lattice relaxation time measurements in two-dimensional NMR imaging. *J. Comput. Assist. Tomogr.* 8:195–199; 1984.
3. Wehrli, F.H.; MacFall, F.R.; Shutts, D.; Breger, R.; Herfkens, R.J. Mechanisms of contrast in NMR imaging. *J. Comput. Assist. Tomogr.* 8:369–380; 1984.
4. Wehrli, F.W.; MacFall, J.R.; Glover, G.H.; Grigsby, N.; Haughton, V.; Johanson, J. The dependence of NMR image contrast on intrinsic and pulse sequence timing parameters. *Magn. Res. Imaging* 2:3–16; 1984.
5. Moran, P.R. A general approach to T_1, T_2 and spin-density discrimination sensitivities in NMR imaging sequences. *Magn. Res. Imaging* 2:17–22; 1984.
6. Perman, W.H.; Hilal, S.K.; Simon, H.E.; Maudsley, A.A. Contrast manipulation in NMR imaging. *Magn. Res. Imaging* 2:23–32; 1984.
7. Young, I.R.; Bailes, D.R.; Collins, A.G.; Guilderdale, D.J. Image options in NMR. Witcofski, R.L.; Karstaedt, N.; Partain, C.L., eds. *NMR imaging, proceedings of an international symposium on nuclear magnetic resonance imaging.* Bowman Gray School of Medicine, Winston-Salem, N.C.: 93–100; 1982.
8. Young, I.R.; Bailes, D.R.; Bydder, G.M. Apparent changes of appearance of inversion-recovery images. *Magn. Res. in Med.* 2:81–85; 1985.
9. Hendrick, R.E.; Nelson, T.R.; Hendee, W.R. Phase detection and contrast loss in magnetic resonance imaging. *Magn. Res. Imaging* 2:279–283; 1984.
10. King, K.F.; Moran, P.R. A unified description of NMR imaging data collection strategies and image reconstruction. *Med. Phys.* 11:1–17; 1983.
11. Moran, P.R. A flow velocity zeugmatography interface for NMR imaging in humans. *Magn. Res. Imaging* 1:197–203; 1982.
12. Moran, P.R.; Moran, R.A. Imaging true motion velocity and higher order motions quantities by phase-gradient-modulation techniques in MRI. Esser; Johnston; Sorenson, eds. *Technology of NMR Soc. Nuc. Med.,* New York, N.Y.:149–163; 1983.
13. Moran, P.R.; Moran, R.A.; Karstaedt, N. Verification and evaluation of internal flow and motion. True magnetic resonance imaging by the phase gradient modulation method. *Radiology* 154:433–441; 1985.
14. Kumar, N.G.; Jackels, S.C.; Karstaedt, N., Moran, P.R. Tissue contrast enhancement with image reconstruction type and selection of TI in inversion recovery MRI. *Book of Abstracts of the Society of Magnetic Resonance in Medicine, Fourth Annual Meeting* (Abstract), 2: pp. 1005–1006, 1985.